HHS Public Access

Author manuscript

*Chem Soc Rev*. Author manuscript; available in PMC 2019 August 28.

Published in final edited form as:

*Chem Soc Rev*. 2018 August 28; 47(17): 6486–6504. doi:10.1039/c8cs00187a.

# Silkworm Silk-based Materials and Devices generated using Bio-nanotechnology

**Wenwen Huang**, **Shengjie Ling**[1,2], **Chunmei Li**, **Fiorenzo G. Omenetto**, and **David L. Kaplan**

[1]Department of Biomedical Engineering, Tufts University, 4 Colby Street, Medford, Massachusetts, 02155, United States

[2]Laboratory for Atomistic and Molecular Mechanics (LAMM), Department of Civil and Environmental Engineering, Massachusetts Institute of Technology, Cambridge, Massachusetts 02139, United States

## Abstract

Silks are natural fibrous protein polymers that are spun by silkworms and spiders. Among silk variants, there has been increasing interest devoted to the silkworm silk of *B. mori*, due to its availability in large quantities along with its unique material properties. Silk fibroin can be extracted from the cocoons of the *B. mori* silkworm and combined synergistically with other biomaterials to form biopolymer composites. With the development of recombinant DNA technology, silks can also be rationally designed and synthesized via genetic control. Silk proteins can be processed in aqueous environments into various material formats including films, sponges, electrospun mats and hydrogels. The versatility and sustainability of silk-based materials provides an impressive toolbox for tailoring materials to meet specific applications via eco-friendly approaches. Historically, silkworm silk has been used by the textile industry for thousands of years due to its excellent physical properties, such as lightweight, high mechanical strength, flexibility, and luster. Recently, due to these properties, along with its biocompatibility, biodegradability and non-immunogenicity, silkworm silk has become a candidate for biomedical utility. Further, the FDA has approved silk medical devices for sutures and as a support structure during reconstructive surgery. With increasing needs for implantable and degradable devices, silkworm silk has attracted interest for electronics, photonics for implantable yet degradable medical devices, along with a broader range of utility in different device applications. This *tutorial review* summarizes and highlights recent advances in the use of silk-based materials in bio-nanotechnology, with a focus on the fabrication and functionalization methods for *in vitro* and *in vivo* applications in the field of tissue engineering, degradable devices and controlled release systems.

## Graphical Abstract

Correspondence to: David L. Kaplan.

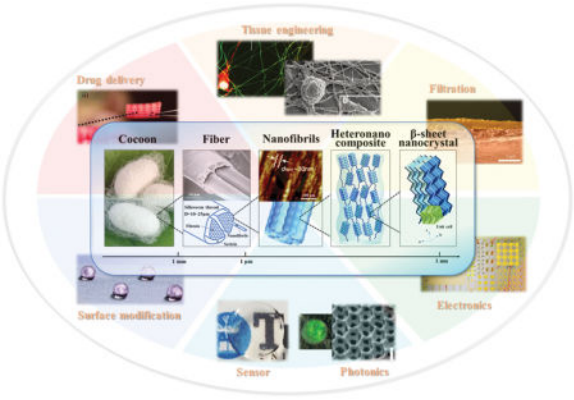


## 1. Introduction

Bio-nanotechnology is an emerging field that sits at the convergence of biology, material science and nanotechnology. This field holds exciting opportunities to foster high-impact advances in bioengineering and medicine. Recent progresses in biochemical engineering, such as genetic engineering, protein engineering, site-specific chemistry, self-assembly and high-throughput screening, enable the optimization, integration and tuning of the functions and properties of biological materials. Advances in nanotechnology, such as high-resolution cryo-electron microscopy, top-down and bottom-up nanofabrication, lab-on-a-chip and microfluidics technology, offer the ability to exploit the structures, functions and processes of biological systems to produce novel functional nanostructured biological materials and systems. Therefore, with the developments of both biotechnology and nanotechnology, synthesizing, assembling and engineering biological molecules with specific functions and properties is a rapidly growing field of bio-nanotechnology for biomedical and high technology applications, such as for diagnostics, medicine, tissue engineering and devices where sustainability and degradability of important.[1]

Fibrous proteins are Nature’s building blocks, conferring structure and function to biological materials. These proteins provide a unique system to study and exploit, as they are simultaneously “biological” (e.g., biocompatible, biodegradable, implantable) and “technological” (e.g., mechanically robust, flexible, micro- and nanostructured, printable, etc.), making them suitable candidates for applications at the interface between these two fields. Most fibrous proteins are linear biopolymers built from a series of up to 20 canonical amino acids. The linear sequence of amino acids in the protein chain (protein primary structure) describes the chemistry of proteins, and thus drives the folding and intra- and intermolecular bonding of protein molecules at nanoscale. Because of the various chemistries among the amino acid side chains, many fibrous proteins are polymorphic and can fold into different secondary structures, depending on the environmental conditions. This unique property of fibrous protein allows engineering the material formats to be achieved through physicochemical approaches. Moreover, proteases recognize specific amino acid sequences (cleavage sites) within the protein chains and catalyze hydrolysis of protein backbone, making fibrous protein a degradable material. The rate of enzymatic cleavage is related to the protein primary structure and protein chain conformation (e.g.,

highly crystallized fibrous protein, such as silk, degrades slowly due to crystallization and orientation, as well as compact structure[2]). The direct utilization and re-engineering of fibrous proteins into biodegradable hierarchical biomaterials offers sustainable methods towards “green” bio-nanotechnological material platforms.[3]

Silk is a unique fibrous protein, providing a versatile polymer template to inspire the design of sophisticated hierarchical architectures from the nanoscale. Due to genetic control of the encoded protein sequence, along with robust mechanical properties, biocompatibility, and biodegradability, this protein has become favorable system with which to study prototype models to emulate tunable designs using bio-nanotechnology. Among silk variants, interest has been devoted to the silkworm silk of *B. mori* due to its availability and desirable properties, such as the ease with which it can be chemically modified, its biocompatibility, its slow rate of degradation *in vivo*, and its ability to be processed into multiple material formats from either aqueous solution or organic solvents.[2] Historically, silkworm silk has been used by the textile industry for thousands of years, due to its excellent physical properties, such as light weight features, high mechanical strength, flexibility, and luster. Recently, due to its biocompatibility, biodegradability and non-immunogenicity, silkworm silk has become a candidate for biomedical uses, and is FDA approved for some medical devices. These include sutures and as a support structure during reconstructive surgery.[4] With an increasing need for implantable devices and sustainable technologies, silkworm silk has also attracted interest for electronics, photonics and filtration systems.[5]

This tutorial review provides an overview of recent progress in the development of silk-based materials using bio-nanotechnology. In the first part of the review, the fundamental properties and production of silk proteins are summarized. Following this section, recent advances in protein engineering are described, with a specific focus on lithography, liquid exfoliation, genetic engineering, self-assembly, and site-specific crosslinking approaches. Finally, the biomedical and technology applications of silk-based materials are highlighted, demonstrating the possibilities for these materials for *in vitro* and *in vivo* applications in the fields of tissue engineering, sustainable devices and controlled release systems.

## 2. Silk in a materials world

### 2.1 Silk: materials overview

**Sequence-structure relationships of *B. mori* silk fibroin—***B. mori*** silk fibroin is the major component of silkworm silk fibers, which consist of 3 major proteins: a heavy chain, a light chain, and a glycoprotein, P25.[2] The heavy chain is 5,263 amino acid residues long, with a molecular weight of 391,367 Da and an isoelectric point of 4.22.[2] It is composed of 45.9% glycine (G), 30.3% alanine (A), 12.1% serine (S), 5.3% tyrosine (Y), 1.8% valine (V), and 4.7% of the other 15 amino acid types.[2] The primary structure of the heavy chain consists of highly repetitive, low-complexity region, bordered by N- and C-termini, in which the repetitive sequence GAGAGS (432 copies) and GAGAGY (120 copies) account for 72% of the low-complexity region.[2] The light chain is 244 amino acid residues long, with a molecular weight of 25,800 Da. The light chain has a less differentiated amino acid composition and non-repetitive sequence. The heavy and light chains are linked by a disulfide bond between Cys-20 of the heavy chain and Cys-172 of the light chain to

form a heavy-light chain complex.[2] The glycoprotein P25 has a molecular weight of 30 kDa. The P25 associates with the heavy-light chain complex mainly by hydrophobic interactions with the heavy chain and helps to maintain the integrity of the heavy-light chain complex.[2]

Structural analysis of silk fibers shows that the formation of various secondary structures in the crystalline and amorphous regions of *B. mori* silk fibroin is directly related to the primary sequence of the silk proteins. The repetitive hydrophobic domains in the *B. mori* heavy chain are mainly composed of the long concatenated blocks of $(GA)_nGX$ of varying lengths and arrangements, which generate the ordered structures and form into crystalline/semi-crystalline domains. For example, the highly repetitive hexapeptide GAGAGS motifs constitute the anti-parallel β-sheets and form the bulk of crystalline regions.[6] The less repetitive hexapeptide GAGAGY motifs constitute the type II β-turns and form the semi-crystalline domains. The tetrapeptides GAAS and GAGS motifs form β-turn structures and serve as the "sheet-breaking" motifs at the C-terminal end of each subdomain.[6] The non-repetitive hydrophilic domains in *B. mori* heavy chain, such as TGSSGFGPYVANGGYSGYEYAWSSESDFGT, generate less ordered structures to form the amorphous or less crystalline matrix in silk fibers.[6] Various investigations revealed that anti-parallel β-sheet nanocrystals play a key role in defining the remarkable mechanical strength of silks by providing stiff ordered cross-linking domains, while the semi-amorphous matrix that consists of β-turn, helix, and random coil structures provide elasticity and physical links between crystalline domains.[6] The *B. mori* light chain is composed of non-repetitive hydrophilic sequences, and it is relatively elastic with little or no crystallinity.

**Hierarchical structures of *B. mori* silk fibers—**Many natural biomaterials exhibit structures on more than one length scale, in which the elements themselves have structural features to form a hierarchical architecture. This structural hierarchy plays an important role in determining bulk materials properties, and thus understanding the effects of hierarchical structure can guide the design of new materials with physical properties that are targeted for specific applications. Silks are highly optimized hierarchical nano-structures with outstanding mechanical properties, thus serving as a source of inspiration for high-performance material designs (Figure 1). On the macroscopic level, the morphological structure of *B. mori* silk fibers possess a core-shell structure, with an inner layer of fibroin and an outer coating of glue-like sericin.[7, 8] The *B. mori* fibroin core consists of two brins (i.e. filaments), each of which displays a triangular cross-section. The sericin gum is about 0.5 to 2 μm thick.[7] The diameter of the silk thread varies across types and specie of silkworm. *B. mori* silk fibers with sericin possess diameters in the range from 10 to 25 μm.[7] On the microscopic level, the morphological structure of *B. mori* silk fibers exhibit a sophisticated hierarchical structure, in which highly organized antiparallel β-sheet nanocrystals are loosely aligned with the fiber axis and dispersed within a semi-amorphous matrix consisting of helices and β-turns.[9] The densely H-bonded β-sheet nanocrystals, which occupy up to 50 – 60% or more of the volume fraction of the fibroin, generate the high tensile strength and modulus in the degummed fiber. In addition, nanoscale confinement of β-sheet nanocrystals, as well as other semi-amorphous structures in silk fibers, also serves a fundamental role in achieving the high mechanical strength.[10] The amorphous molecular chains, which adopt random coil, helix or β-turn structures, bridge

different β-sheet nanocrystals and give lateral strength and allow elasticity through large deformations.[10]

**Properties of *B. mori* silk materials—**From a materials science perspective, silkworm silk has excellent mechanical properties such as remarkable strength and toughness (Table 1), offering unlimited opportunities for the fabrication, functionalization and processing of robust biomaterials.[4] In terms of stiffness, silkworm silks are superior to commonly used polymeric degradable biomaterials such as collagen and polylactic acid (PLA). The toughness of silk fibers is greater than the best synthetic materials, including Kevlar. In addition to the impressive mechanical properties, silkworm silk is also a biodegradable material. In general, silk degradation is mediated by enzymes (e.g., protease XIV).[2] The degradation rate of silk can be altered by the processing techniques, as well as post-processing treatments (e.g., the degradation rate decreases with an increase in overall β-sheet content). The *in vivo* degradation rate of silk also depends on the implantation site and mechanical environment.[2] Due to the unique mechanical properties and enzymatic degradability, silk fibroin is considered promising candidate biopolymer for biomedical applications.

Recent progress in material processing has led to the transformation of *B.mori* silk into a variety of new material formats, including films, conformal coatings, hydrogels, nano-fibers, 3D porous sponge and scaffold (Table 2). Among the many possible material forms, silk films are of particular interest for optics and photonics applications because of the transparency (over 90% transmission across the visible range) and surface flatness (surface roughness rms <5 nm).[12] Silk hydrogel, fiber mat, sponge and scaffold are of particular interest for tissue engineering because of their tunable mechanical properties and for drug release because of the available aqueous processing methods for silks.[4]

## 2.2 Production of silk proteins: sericulture and bioengineering

With advances in molecular biology and biotechnology, silk proteins have been synthesized using different host systems.[2, 14, 15] For example, native silk proteins, such as regenerated silk fibroin (RSF), are extracted from native silk fibers that are spun by arthropods.[2] Functionalize silk fibers are produced by transgenic silkworms.[15] Bioengineered silk proteins, also called recombinant silks, are bio-synthesized in heterologous hosts, such as bacteria, yeasts, mammalian cells, plant cells and insect cells.[14] Generating silk proteins in large scale with cost-effective methods is essential for their applications as functional biological materials. Among various silk protein synthesis methods, two methods are industrially scalable: silk fibroin extraction and bioengineered silk fermentation, and thus they have become the main synthesis methods for silk proteins. Additional options, such as transgenic animals and transgenic plants, can also provide suitable quantities of recombinant silk proteins pending scale up process optimization and cost reduction.[15]

**Silk Fibroin Extraction—**Due to large-scale cultivation of silkworms for the textile industry, there are abundant and reasonable cost sources for *B. mori* silkworm silk fiber. Native *B. mori* silkworm silk fiber is composed of silk fibroin protein core coated by sericin proteins, which was previously reported to elicit an immune response.[2] Therefore, removal

of sericin from silkworm silk is necessary to prepare non-allergic and non-cytotoxic silk-based materials for medical applications.

In general, *B. mori* silk regeneration is a three-step process, including degumming, rehydration and dialysis (Figure 2a). First, in degumming, *B. mori* silkworm cocoons are boiled in a 0.02 M $Na_2CO_3$ solution to remove sericin proteins; silk proteins undergo partial degradation during this process dependent upon the length of the degumming time. For example, samples that were degummed for 30 minutes had a broad molecular weight distribution near 100 kDa. This value increases for shorter degumming times or decreases when degummed for longer times. The molecular weight of RSF in turn affects the processing of the regenerated silks and the mechanical properties of silk-based materials generated from these proteins.[2] Second, in the dehydration step, the degummed fibers are dissolved in 9.3 M LiBr solution at 60°C for 4 h to enable rehydration of the proteins.[2] The hydrogen bonded crystalline structure in silk proteins are disrupt in this process, providing a consistent starting material for downstream silk materials fabrication and functionalization. Finally, the LiBr is dialyzed away, resulting in an aqueous solution of pure regenerated silk fibroin (RSF) ready to use.[2] Other options for the reverse engineering of silk fibers to aqueous silk solutions are also available and accomplish somewhat similar outcomes as the process described above.

**Bioengineered silk fermentation—**Genetic engineering provides a powerful tool to construct silk protein with high degree of molecular definition. In contrast to extraction methods, the sequence and molecular weight of bioengineered proteins can be strictly controlled by the genetic template, leading to monodisperse, precisely defined biopolymers.

Current strategies for the production of bioengineered silks can be summarized in three steps: plasmid construction, expression and purification (Figure 2b). To construct expression plasmids for recombinant silks, a variety of cloning strategies have been used toward this goal: step by step directional ligation and recursive directional ligation were used to produce new silk-related genes with control of size,[16] and concatemerization was preferred for the construction of gene libraries.[17] Once the plasmid sequences are confirmed, the plasmid is transformed into a bacterial host (commonly *E. coli*) for the expression of silk proteins. The main purification method used for recombinant silk proteins has been metal chelate affinity chromatography, which utilizes the highly specific interaction between nickel-charged nitrilotriacetic acid resin (Ni-NTA resin) and histidine tag for target protein isolation.[16] Inverse temperature cycling is preferred for the purification of some silk proteins with elastin domains, due to its low cost and ease of scale-up.[18] The key advantages of bioengineered silk proteins include tight control on silk sequence and molecular weight, ability to tailor its sequence, and versatility in protein chemistry.[16] The process remains limiting in terms of protein yield when generating high molecular weight silks, when cloning full-length silk genes, or when large-scale production of silk proteins is needed.[16] Industrialization of the process, however, is underway to overcome these limitations, using a range of host expression systems apart from the *E. coli* described above.

## 3. Engineering Silks

Recent advances in nanostructured biomaterials and biomedical microelectromechanical systems (bio-MEMs) have opened up new opportunities in a variety of applications, ranging from healthcare and medicine to sustainable high technology devices.[5] Top-down and bottom-up approaches are the two main nanofabrication methods to create structures at the nano level. Top down nanofabrication generally relies on the transformation or rearrangement of bulk materials into nanopatterned structures. Top-down approaches that are commonly used for silk materials include soft-lithography, photolithography, ion beam lithography, nanoimprinting, liquid exfoliation, and electrospinning. The key advantage of top-down approaches is the ability to precisely pattern desired material features in an exact location. On the other hand, bottom-up nanofabrication is based on molecular assembly, in which materials are generated via chemical or physical forces or interactions operating at the nanoscale, ultimately resulting in ordered domains on the nanoscales. Some relevant tools that complement bottom-up approaches commonly used for silk materials include recombinant DNA technology that direct self-assembly. The key advantage of bottom-up approaches is the ability to achieve feature resolution down to atomic precision based on chemistry, while the most significant disadvantage is the limitation of large scale uniformity when scaling up.

### 3.1 Nanolithography

Nanolithography is a branch of nanotechnology that involves etching, writing or printing to modify a material surface with structures at the microscopic level. This process is conventionally used in the manufacture of semiconductor chips for electronic devices. Over the last decades, nanolithography has been adapted for bio-MEMs, leading to significant advances in different fields of medicine and biology.

Soft lithography is a convenient, effective, and low-cost top-down nano-fabrication method to replicate nanostructures using elastomeric molds (Figure 3a). *B. mori* regenerated silk fibroin solution (RSF) is a useful starting biomaterial for soft lithography. By casting the aqueous RSF solution on nanostructured surfaces, the topographies can be replicated onto free-standing silk films with feature sizes of less than 10 nm.[12] The resulting patterned silk films possess high mechanical strength, flexibility, high surface quality (surface roughness rms <5 nm) and optical transparency (over 90% transmission across the visible range).[12] Using this approach in combination with the optical transparency of silk films, a variety of soft optics and flexible devices can be fabricated.[12, 20] In contrast to traditional nanofabrication techniques which often require complex lithographic steps and the use of toxic chemicals, this silk-based soft lithography casting process is completed in the absence of additional harsh chemicals, salts, or high temperature and pressures, providing a simple, sustainable and versatile route for the fabrication of silk-based biomedical devices, with options to include temperature-sensitive therapeutics depending on the application.[20]

Nanoimprint lithography is a rapid and high-throughput top-down nano-fabrication technique to transfer sub-100 nm features onto a flat material surface using a hard master mold at elevated temperature and pressure (Figure 3b). The choice of nanoimprinting temperature depends on the glass transition temperature ($T_g$) of the silk fibroin films, which

is tunable by the water content in the silk.[21] For example, silk films prepared at ambient humidity (~35%) have a glass transition temperature around 100°C, and therefore can be nanoimprinted by a heated hard mold at 100°C, 30–50 psi for 5 seconds. Water-saturated silk films have a $T_g$ around ambient temperature, and therefore can be nanoimprinted at room temperature. A structure stabilization step, such as methanol vapor exposure, is required for room temperature nanoimprinting to lock the nano-pattern on silk film surface by formation of β-sheets.[21] Additionally, crosslinked silk films can be used to imprint noncrosslinked films in sequential fashion, achieving both positive and negative tone nanoscale replicas.[22] Using this approach, biophotonics or materials containing bioactive molecules, have also been fabricated.[21] The ability to perform nanoimprinting on silk films increases the quality and throughput of nanostructured silk materials in comparison to casting methods.

Ion beam lithography and electron-beam lithography use an accelerated beam of electrons or ion to create nanostructures (Figure 3c). Due to its polymorphic nature, silk can be used as a positive or negative resist in electron-beam lithography.[23] For positive resist fabrication, the crystallized silk film is water-resistant and the electron-beam exposure degrades specific regions on the silk surface into water-soluble polypeptides to create nanostructures. For negative resist fabrication, the amorphous silk film is water-soluble and the high-energy electron beams cause amorphous-to-helix assembly of silk fibroin in amorphous silk films, rendering specific regions in silk proteins insoluble. Nanophotonic lattices and super-hydrophobic fabrics have been fabricated with these approaches.[23, 24] Electron-beam lithography provides a maskless patterning technique that generates arbitrary patterns at a spatial resolution of 10 nm,[25] while the technique suffers from some inherent limitations, notably cost and speed.

Photolithography is an efficient and cost-effective top-down nano-fabrication technique to create micro-scale features on silk, by defining patterns on the material surface using light (Figure 3d). Silk exhibits a strong absorption of deep ultraviolet (DUV) light at a wavelength of 193 nm.[26] In positive-tone photolithography, the crystallized silk film is water-resistant and the DUV exposure degrades specific regions on silk film surfaces into water-soluble polypeptides to create micro-scale structures.[26] Using this approach, the bioactive dopants can be protected from DUV irradiation to minimize the loss of their biofunction.[26] This process is entirely water-based, offers a relatively simple way to generate microscale patterns and facilitate the fabrication of patterned silk films with bioactive dopants.

### 3.2 Confined Alignment

The degree of molecular alignment and the degree of crystallinity are both important in controlling the properties of polymeric materials, especially mechanical properties. Inspired by this concept, mechanical tension-mediated directed assembly was developed to generate hierarchical nanofibrillar structures (Figure 4).[29] In this process, macroscopically patterned soft silk hydrogels with low β-sheet and α-helix contents were mechanically aligned by either gel contraction through submersion in a mixture of water and ethanol or by direct deformation of a PDMS substrate housing the gels. The aligned hydrogels were treated by critical point drying (CPD) where β-sheet physical crosslinking in the silk was induced. This

fabrication protocol leads to the generation of oriented nanofibrillar networks within predesigned macroscopic structures, which possess high mechanical strength (the web formed in this process sustained more than 4,000 times its weight).[29] This method simultaneously controls macroscale geometry, micromechanical constraints and solvent removal dynamics, and enables the design and engineering of biopolymer-based hierarchical constructs with control at multiple length scales. The ease of doping such structures also enables new classes of designer structures with tunable properties.

### 3.3 Liquid exfoliation

Liquid exfoliation is a top-down approach that can be used to isolate important structural elements from sophisticated hierarchical architectures. This method is conventionally used to fabricate nanostructured 2D materials, such as single layer graphene, in organic solvents. Inspired by the liquid exfoliation of graphene, a new liquid exfoliation method to directly exfoliate silk fibers at the single silk nanofibril (SNF) level was developed (Figure 5).[30] This process used a combination of partial chemical dissolution and physical ultrasonic dispersion to obtain SNFs with diameters of 20 ± 5 nm and contour lengths of up to 500 nm.[30] The top-down liquid exfoliation method, which directly exfoliates SNFs from degummed silks, can preserve the native structural elements and features from silk fibers with the aim to re-arrange them at the nanofibril level for enhanced properties. In particular, the SNFs were re-arranged into well-structured membranes by a vacuum-assisted filtration process. The new SNF membranes were used as optical and electronic devices with potential for advanced materials toward tissue engineering, optical devices, nanoelectronics, and biosensors.[30]

### 3.4 Electrospinning

Electrospinning is a relatively simple and effective method to produce uniform continuous fibers with diameters ranging from the nanoscale to the microscale. These micro/nanofibers in the form of nonwoven mats have been used widely in biomaterials, tissue engineering and drug delivery. Notably, nanostructured flexible fibers can be produced by optimization of the electrospinning set-up. In particular, an all-aqueous coaxial electrospinning nanofabrication method for the production of flexible core-shell structured nanofibers was developed to obtain silk fibroin (SF) and silk-elastin-like protein (SELP) (Figure 6). SF-SELP core-shell structured nanofibers provide interesting utility in biomaterial systems due to the functional layer on the surface of the SF fibers.[31]

### 3.5 Genetic engineering

Genetic engineering provides a bottom-up approach to biosynthesize recombinant proteins with a high degree of molecular definition. The three main steps to produce bioengineered silks can be summarized as plasmid construction, expression and purification. Through appropriate mutations in the genetic template during plasmid construction, the properties and functionalities of bioengineered proteins and their sequence-structure-function relationships can be optimized for specific applications. This bioengineering approach facilitates systematic studies to correlate sequence with molecular architecture and functionality, and also enables the construction of new silks *de novo* through the addition of key motifs from other proteins to introduce new functions. In particular, elastin motifs were

incorporated with silk motifs through recombinant DNA technology to develop stimuli-responsive yet a robust protein library of silk-elastin-like proteins (SELPs) (Figure 7).[17] These proteins, which do not exist in nature, possess stimuli-responsive features from elastin motifs and the mechanical stiffness from silk motifs. SELPs were then fabricated into nanoparticles and microstructured smart hydrogels for drug delivery and bio-actuators.[18, 32] The use of genetic engineering to enhance material properties paves the way for tailoring protein materials for tissue engineering, biosensors and many other material-centric applications.

### 3.6 Self-assembly

Self-assembly is a bottom-up approach in which components spontaneously form ordered patterns or hierarchical structures without human intervention. Proteins can self-assemble into various nanostructures, and this process is generally driven initially by nonspecific forces, such as hydrophobic interactions, and then fine-tuned by more specific interactions, such as hydrogen bonding. Silk proteins are hierarchical, amphiphilic, block copolymers composed of alternating hydrophobic and hydrophilic blocks, and this amphiphilic pattern drives the self-assembly of spherical micellar structures in the glands of the organism during silk formation (Figure 8a). The micellar structure is about 100–200 nm, containing a hydrophobic core of crystalline-amorphous domains and a hydrophilic shell of the terminal domains.[33] Silk fiber spinning is also a natural self-assembly process. As the fibroin micelles passes along the processing duct in the animal, a variety of chemical and physical stimuli, such as a decrease in pH, increase in ion exchange and silk solution concentration, and shear force, cause the rapid irreversible transition of silk proteins from the solution state (Silk I) to an insoluble form dominated by anti-parallel beta sheet crystals (Silk II), leading to the formation of self-assembled hierarchically structured silk fibers (Figure 8b).[33] Inspired by the natural fiber spinning process, artificial spinning and biomimetic spinning have also been developed to fabricate silk fibers via an aqueous-based self-assembly process, thereby providing an eco-friendly and sustainable approach to produce silk materials without the need to use harsh chemicals or crosslinkers. [34, 35]

### 3.7 3D Printing

3D printing is a bottom-up additive manufacturing technology where structures are built up in a layer-by-layer fashion, with precision spanning multiple length scales. This technique allows the formation of custom geometries that are difficult or impossible to manufacture with conventional fabrication techniques. The recent success in developing bio-inks which can encapsulate and protect stem cells during the 3D printing process also opens the door for direct printing of human organs. Regenerated silk fibroin (RSF) is a unique bio-ink for 3D printing due to its polymorphic nature, absence of need for chemical or photochemical crosslinking and biocompatibility. A 3D printing method using one-step gelation of RSF within a nanoclay suspension of laponite was developed to fabricate 3D biomaterials with complex structures down to the microscale, with potential for utility in tissue regeneration (Figure 9).[36]

### 3.8 Crosslinking

Crosslinking is a process of joining two or more molecules by chemical bonds. This post-synthesis protein modification method is crucial for changing the polymorphism of silk for nanofabrication and the direct formation of mico/nanostructures. Crosslinking approaches can be classified into two main groups: i) physical methods, which use temperature, shear force and electric fields to induce hydrogen bonded β-sheets for crosslinking; and ii) chemical methods, which use protein chemistry to form ionic and covalent bonds for crosslinking.[2] Water annealing and alcohol immersion are commonly used approaches to form β-sheet crystals, as physical crosslinkers based on hydrogen bonding.[2] Water annealing is a process in which the silk materials are incubated in a humid environment for isothermal crystallization without addition of hash chemicals or salts. Alcohol immersion is a simple and rapid method, it can embrittle the silk materials and also often destroy the biological activity of entrained bioactive substances if present in the silk material, in contrast to the water annealing approach. Enzyme catalyzed chemical crosslinking was developed to fabricate nanostructured hydrogels. In particular, a new method for covalently crosslinking tyrosine residues in silk proteins and SELPs, via horseradish peroxidase and hydrogen peroxide, generated elastic hydrogels with tunable properties (Figure 10). These materials offer tunable mechanics, stimuli responsive, and swelling properties. It should be noted that the elastic gels will stiffen with time, where the rate and extent of changes depends on the degree of crosslinking, the solution in which the hydrogels are placed, and the presence of copolymers in the reactions.[37]

## 4. Applications of Silk-based Materials in Bio-nanotechnology

### 4.1 Tissue Engineering

In tissue engineering, biomaterial scaffolds play a pivotal role by defining the three-dimensional extracellular matrix templates for tissue regeneration. Besides excellent biocompatibility and biodegradability, matching mechanical properties to native tissue extracellular matrix is a primary consideration during the selection of biomaterials. In particular, scaffold stiffness has a significant impact on the differentiation of stem cells and maintenance of cell phenotype during cell culture.[38] In addition, to matched mechanical properties, a useful tissue engineering scaffold should also provide suitable macropores and nanofibrous structure, similar to the extracellular matrix, to induce desired cellular activities and to guide tissue regeneration.

Silk hydrogels are attractive biomaterials for tissue engineering applications, as their stiffness can be fine tuned and they can incorporate growth factors and other cell signaling factors to optimize cell functions.[38, 39] The microstructured and elastic silk hydrogels described above supported stem cell growth and proliferation for greater than 3 weeks. These hydrogels have also been used for stem cell encapsulation and for *in vivo* implants.[38] Aligned silk nanofibers fabricated by electrospinning provide topographical templates leading to elongated and oriented cellular morphologies, which may provide interesting avenues to use silk fiber scaffolds for the *de novo* engineering of structurally aligned tissues. For example, aligned silk nanofibers have been used for the regeneration of nerves (Figure 11).[40] These nanofibers were loaded with brain-derived neurotrophic factor (BDNF), ciliary

neurotrophic factor (CNTF) or both to enhanced cell function without impact to the structure. The results of this work demonstrated the successful rescue of retinal ganglion cells (RGC) death and enhance regeneration using a biofunctionalized electrospun material, with prospective to serve as promising implants for optic-nerve-trauma rescue.[40]

### 4.2 Drug Delivery

Silk-based biomaterials have been utilized as sustainable drug delivery vehicles for a wide range of bioactive molecules including genes, small molecules, and drugs. For each class of molecule, various silk nanotechnologies have been applied for the delivery and controlled release.

Microneedles are a relatively simple, minimally invasive and painless approach to deliver drugs across the skin, compared to hypodermic needles. Silk-based biomaterials offer beneficial properties for the design and fabrication of silk microneedles, including robust mechanical properties, aqueous-based ambient processing options, biocompatibility, controllable biodegradation, and noninflammatory properties. Soft-lithography was utilized to obtain high aspect ratio silk microneedles using room temperate aqueous processing (Figure 12a).[41] These mild fabrication conditions allowed for bulk loading of temperature-sensitive drugs such as peptides, antibiotics and vaccines, or temperature-labile therapeutics, into the silk microneedles. Additionally, controlled release from microneedles was also achieved by adjusting the post-processing conditions through control of silk protein secondary structure, to adjust the degradation rate and drug diffusion properties.[41] The design, shape and geometry of microneedles was further refined and studied in terms of microneedle shapes and mechanical properties.[28] The water vapor treated cone-shaped microneedles had superior mechanical properties (400 mN/needle) than pyramid shaped needles (175 mN/needle). The mechanical properties of the microneedle patches were also improved by loading the needles with silk microparticles (720 mN/needle). Drug release was further enhanced by coating microneedles with a thin dissolvable drug layer.[28] The microneedles were tested on human cadaver skin and drugs were delivered successfully. The various attributes demonstrated for these devices suggest that silk-based microneedle systems can provide significant benefit for transdermal drug delivery.

Silk-based nano- and micro-particulate systems have also been used in biomedical and pharmaceutical applications (Figure 12b,c). Nanospheres can penetrate through small capillaries, across physiological barriers and be incorporated into cells. Therefore, silk-based nanospheres for drug-delivery have been studied for treating various diseases, including cancer. Early clinical results indicated that nanoparticle therapeutics showed enhanced efficacy compared to free chemotherapeutics, while simultaneously reducing side effects, due to properties such as more targeted localization in tumors and active cellular uptake.[32] Microspheres are more generally used as depot drug carriers for long-acting delivery and they usually administered intramuscularly or subcutaneously. The self-assembly of amphiphilic silk molecule as SELPs, can be triggered by adding hydrophobic molecules to form the core of micellar-like nanoparticles.[42] The diameter of nanoparticle therapeutics for cancer should be in the range of 10 to 150 nm to cross the endothelial barrier, and nanoparticles formed by SELPs using the methods described above are in the 20 to 150nm

range. Therefore, the SELP nanoparticles have potential to be used as drug delivery vehicles.[42] Silk micro- and nanospheres with controllable sizes and changeable shapes were fabricated using poly(vinyl alcohol) (PVA).[43] PVA was used as a continuous phase to separate the silk into micro- and nanospheres in silk/PVA blend films. Varying silk and PVA concentrations or applying ultrasonication to the blend solution was used to control sphere size and distribution. Spindle-shaped microspheres were obtained by stretching the blend films. The reported preparation methods were simple, time and energy efficient, and amenable to a wide range of drugs, and thus should be useful for the preparation of silk-based drug delivery systems.[43]

### 4.3 Nanostructured Optics

Silk-based biomaterials have been utilized in optical materials due to favorable properties, such as mechanical robustness, transparency, surface flatness and degradability. With the development of both soft-lithography and nanoimprinting processes, geometries and topologies can be replicated down to tens of nanometers for biophotonic applications using silk fibroin solutions and films.[44] The incorporation of metal nanoparticles in silk also opens up a novel way to fabricate nanostructured biomaterials for biophotonic devices.[45, 46]

A photonic crystal is a periodic optical nanostructure that manipulates photons within small volumes to exhibit structural color based on periodic nanopatterns. Controlled fabrication of inverse opals, a type of 3D photonic crystal, was demonstrated from silk fibroin (Figure 13a).[44] Controlled color changes of silk inverse opals was also demonstrated, both by varying the size of the PMMA spheres and by filling the voids with acetone. The silk inverse opals are biocompatible and show promise as active layers for resorbable label-free biosensing and used to track changes in biological systems during tissue culture.[47] These silk inverse opals substrates visually tracked substrate degradation upon exposure to proteases during tissue digestion, as well as protein deposition during the growth of mesenchymal stem cells on the opals (Figure 13b). Silk protein has been used as a biopolymer substrate for flexible photonic devices due to its attractive mechanical and optical properties. ZnO nanorod array hybrid photodetectors on Au nanoparticle-embedded silk protein were fabricated for flexible optoelectronics.[46] These novel ZnO nanorod array photodetectors on a natural silk protein provide a platform to realize flexible and self-powered bio-photonic devices for medical applications (Figure 13c and 13d).[46]

### 4.4 Electronics

Flexible electronic devices are necessary for applications involving unconventional interfaces, such as soft and curved biological systems, where traditional silicon-based electronics present a mechanical mismatch.[48] Silk-based materials, due to their flexibility and biocompatibility, are suitable candidates for advanced flexible electronic devices. Unlike traditional wafer-based technologies, laminating such devices onto the skin leads to conformal contact and adequate adhesion with the curvilinear surfaces of various organs and effective measurements of electrical activity produced by these organs. The fabrication of flexible silk-based electronics systems incorporating electrophysiological, temperature, and strain sensors was demonstrated in order to measure the electrical activity produced by the heart, brain, and skeletal muscles (Figure 14a).[48] More recently, the fabrication of fully

dissolvable wireless heating devices was demonstrated, consisting of a serpentine resistor and a power-receiving coil, both made of Mg, on the silk substrate (Figure 14b). The Mg heater was protected by encapsulation in a silk “pocket”, which can be used to design the device lifetime. The device could be remotely activated for thermal treatment in the infection area, harmlessly dissolving after infection abatement. Advances in silk-based electronic devices would open new avenues for employing biomaterials in the design and integration of high-performance, bio-integrated electronics for future applications in consumer electronics, computing technologies, and biomedical diagnosis, as well as human-machine interfaces.

### 4.5 Sensors

Recent trends in biomaterial designs have evolved from static to dynamic, bio-responsive systems, to address broader biomedical needs for smart materials. Silk-based materials provide a unique opportunity for tunable designs of dynamic biopolymer systems, due to the genetic basis of sequence control and thus precise chemistry, molecular weight, and chirality control. Harnessing silk proteins to generate stimuli-responsive biomaterials based on protein folding-unfolding for biomedical applications offers tremendous opportunities for fine tuning control, responses, and utility, such as for biosensors and controlled drug delivery devices. Anew family of genetically engineered SELPs with encoded enzymatic crosslinking sites was generated for a new generation of stimuli-responsive shape-changing, yet robust hydrogels (Figure 15).[18] The resultant SELP hydrogels exhibited reversible changes in microstructure, optical transparency, and mechanical properties upon exposure to designed target stimuli, such as temperature, pH, and certain biological signals. The development of these dynamic protein hydrogels based on SELPs suggests new possibilities for using these hydrogels as biosensors. The insight gained will also allow enhanced understanding of structure-function relationships with protein designs, thus guiding genetic designs of dynamic hydrogels that respond predictably to virtually any desired environmental input to trigger changes in the material.

### 4.6 Filtration

Membranes for water treatment have developed to address global challenges of water pollution and to remove molecular level contaminants. A variety of sustainable materials and novel fabrication methods have been developed to improve the purification efficiency of these membranes. Liquid-exfoliated silk nanofibrils (SNFs) were utilized to generate filtration membranes with high water flux and efficient separation for dyes, proteins, and nanoparticles.[30] The SNF membranes are sustainable, and less expensive compared to existing commercial membranes. Multilayer architectures in water purification membranes enable increased water throughput, high filter efficiency, and high molecule loading capacity. Highly ordered multilayer membranes with nanoporous features were fabricated by combining protein self-assembly and in situ biomineralization (Figure 16).[50] This biomimetic design and synthesis of functional silk nanofibrils (SNF) and hydroxyapatite (HAP) materials established a paradigm that could lead to large-scale, low-cost production of multilayer materials with efficiency for water purification and with applications in wastewater treatment and biomedicine.

### 4.7 Surface modification

Due to mechanical weakness of silk in wet conditions, silk needs to have water resistance and super-hydrophobicity properties. A method was developed to fabricate nanostructured, super-hydrophobic, silk fabrics using the ion beam treatment of oxygen etching and subsequent ion beam deposition of a fluorinated diamond-like carbon (Figure 17).[24] The fabricated super-hydrophobic silk fabrics had a static contact angle of 170° and a shedding angle of less than 5°. This process can create super-hydrophobicity on one side of the silk fabric, while the other side remains intact as a more hydrophilic, water absorbing system to obtain asymmetric wettability. The production of super-hydrophobic silk fabric without the loss of the unique silk properties could be useful for breathable, self-cleaning textiles.

## 5. Summary and Outlook

Silk-based biomaterials have been exploited as a sustainable, biodegradable material platform that can be used in a broad scope of biomedical applications, such as medicine, biotechnology and filtration. The mechanical robustness, transparency and surface flatness of silk films are compelling features for photonics and electronics applications. With advances in nanotechnology, new and innovative silk-based material formats are being developed, including nanoparticles, nanofibers, nano-pattered films, hydrogels and aligned scaffolds. The direct utilization and re-engineering of silk-based biomaterials into medical and technological material platforms is already underway in many laboratories and offers a path forward for “green bio-nanotechnology”. The modular nature of silk proteins are also attractive features for the design new silks *de novo* from the atomic scale through biotechnology approaches, thus new functions can be incorporated into silks. There are no other synthetically or biologically derived polymer systems that offer this range of useful material properties and biological interfaces. Therefore, silk remains as a model biopolymer to study and also a prime candidate for bio-devices. Challenges, such as batch-to-batch variation and scale-up processing engineering for the fabrication of these materials remains to be fully vetted as the field moves forward.

## Acknowledgments

The authors acknowledge the financial support of the NIH (Grant U01 EB014976), Tissue Engineering Resource Center (Grant NIH P41 EB002520), the ARO (W911NF-17-1-0384), the ONR (N00014-16-1-2333), and the AFOSR (FA9550-11-1-0199).

## References

1. de la Rica R, Matsui H. Chemical Society Reviews. 2010; 39:3499–3509. [PubMed: 20596584]
2. Rockwood DN, Preda RC, Yucel T, Wang XQ, Lovett ML, Kaplan DL. Nature Protocols. 2011; 6:1612–1631. [PubMed: 21959241]
3. Guilbert S, Morel MH, Gontard N, Cuq B. Feedstocks for the Future: Renewables for the Production of Chemicals and Materials. 2006; 921:334–350.
4. Altman GH, Diaz F, Jakuba C, Calabro T, Horan RL, Chen JS, Lu H, Richmond J, Kaplan DL. Biomaterials. 2003; 24:401–416. [PubMed: 12423595]
5. Omenetto FG, Kaplan DL. Science. 2010; 329:528–531. [PubMed: 20671180]
6. Malay AD, Sato R, Yazawa K, Watanabe H, Ifuku N, Masunaga H, Hikima T, Guan J, Mandal BB, Damrongsakkul S. Scientific reports. 2016; 6:27573. [PubMed: 27279149]

7. Shao Z, Vollrath F. Nature. 2002; 418:741–741. [PubMed: 12181556]
8. Qi Y, Wang H, Wei K, Yang Y, Zheng RY, Kim IS, Zhang KQ. International Journal of Molecular Sciences. 2017; 18:237.
9. Xu GQ, Gong L, Yang Z, Liu XY. Soft Matter. 2014; 10:2116–2123. [PubMed: 24652059]
10. Keten S, Xu ZP, Ihle B, Buehler MJ. Nature Materials. 2010; 9:359–367. [PubMed: 20228820]
11. Xia XX, Qian ZG, Ki CS, Park YH, Kaplan DL, Lee SY. Proceedings of the National Academy of Sciences of the United States of America. 2010; 107:14059–14063. [PubMed: 20660779]
12. Omenetto FG, KapLan DL. Nature Photonics. 2008; 2:641–643.
13. Koh LD, Cheng Y, Teng CP, Khin YW, Loh XJ, Tee SY, Low M, Ye E, Yu HD, Zhang YW, Han MY. Progress in Polymer Science. 2015; 46:86–110.
14. Xia XX, Xu QB, Hu X, Qin GK, Kaplan DL. Biomacromolecules. 2011; 12:3844–3850. [PubMed: 21955178]
15. Teramoto H, Amano Y, Iraha F, Kojima K, Ito T, Sakamoto K. Acs Synthetic Biology. 2018; 7:801–806. [PubMed: 29480717]
16. Huang WW, Ebrahimi D, Dinjaski N, Tarakanova A, Buehler MJ, Wong JY, Kaplan DL. Accounts of Chemical Research. 2017; 50:866–876. [PubMed: 28191922]
17. Wang Q, Xia X, Huang W, Lin Y, Xu Q, Kaplan DL. Advanced Functional Materials. 2014; 24:4303–4310. [PubMed: 25505375]
18. Huang WW, Tarakanova A, Dinjaski N, Wang Q, Xia XX, Chen Y, Wong JY, Buehler MJ, Kaplan DL. Advanced Functional Materials. 2016; 26:4113–4123. [PubMed: 28670244]
19. Lin S, Ryu S, Tokareva O, Gronau G, Jacobsen MM, Huang W, Rizzo DJ, Li D, Staii C, Pugno NM, Wong JY, Kaplan DL, Buehler MJ. Nature Communications. 2015; 6:6892.
20. Tao H, Hwang SW, Marelli B, An B, Moreau JE, Yang MM, Brenckle MA, Kim S, Kaplan DL, Rogers JA, Omenetto FG. Proceedings of the National Academy of Sciences of the United States of America. 2014; 111:17385–17389. [PubMed: 25422476]
21. Amsden JJ, Domachuk P, Gopinath A, White RD, Dal Negro L, Kaplan DL, Omenetto FG. Advanced Materials. 2010; 22:1746–1749. [PubMed: 20496408]
22. Brenckle MA, Tao H, Kim S, Paquette M, Kaplan DL, Omenetto FG. Advanced Materials. 2013; 25:2409–2414. [PubMed: 23483712]
23. Kim S, Marelli B, Brenckle MA, Mitropoulos AN, Gil ES, Tsioris K, Tao H, Kaplan DL, Omenetto FG. Nature Nanotechnology. 2014; 9:306–310.
24. Oh JH, Ko TJ, Moon MW, Park CH. Rsc Advances. 2014; 4:38966–38973.
25. Qin N, Zhang SQ, Jiang JJ, Gilbert Corder S, Qian ZG, Zhou ZT, Lee W, Liu KY, Wang XH, Li XX, Shi ZF, Mao Y, Bechtel HA, Martin MC, Xia XX, Marelli B, Kaplan DL, Omenetto FG, Liu MK, Tao TH. Nature Communications. 2016; 7:8.
26. Park J, Lee SG, Marelli B, Lee M, Kim T, Oh HK, Jeon H, Omenetto FG, Kim S. Rsc Advances. 2016; 6:39330–39334.
27. Stinson JA, Raja WK, Lee S, Kim HB, Diwan I, Tutunjian S, Panilaitis B, Omenetto FG, Tzipori S, Kaplan DL. Acs Biomaterials Science & Engineering. 2017; 3:360–369.
28. Raja WK, MacCorkle S, Diwan IM, Abdurrob A, Lu J, Omenetto FG, Kaplan DL. Small. 2013; 9:3704–3713. [PubMed: 23653252]
29. Tseng P, Napier B, Zhao SW, Mitropoulos AN, Applegate MB, Marelli B, Kaplan DL, Omenetto FG. Nature Nanotechnology. 2017; 12:474–480.
30. Ling S, Li C, Jin K, Kaplan DL, Buehler MJ. Advanced Materials. 2016; 28:7783–7790. [PubMed: 27352291]
31. Zhu J, Huang W, Zhang Q, Ling S, Chen Y, Kaplan LD. Materials. 2016; 9:221.
32. Huang W, Rollett A, Kaplan DL. Expert Opinion on Drug Delivery. 2015; 12:779–791. [PubMed: 25476201]
33. Jin HJ, Kaplan DL. Nature. 2003; 424:1057–1061. [PubMed: 12944968]
34. Ling S, Qin Z, Li C, Huang W, Kaplan DL, Buehler MJ. Nature Communications. 2017; 8:1387.
35. Sparkes J, Holland C. Nature Communications. 2017; 8:594.

36. Maria TAD, Rodriguez J, Eliad, Cohen WH, Omenetto Fiorenzo, Kaplan David L. Acta Biomaterialia. 2018; 71:379–387. [PubMed: 29550442]
37. Raia NR, Partlow BP, McGill M, Kimmerling EP, Ghezzi CE, Kaplan DL. Biomaterials. 2017; 131:58–67. [PubMed: 28376366]
38. Partlow BP, Hanna CW, Rnjak-Kovacina J, Moreau JE, Applegate MB, Burke KA, Marelli B, Mitropoulos AN, Omenetto FG, Kaplan DL. Advanced Functional Materials. 2014; 24:4615–4624. [PubMed: 25395921]
39. Bienert M, Hoss M, Bartneck M, Weinandy S, Boebel M, Jockenhoevel S, Knuechel R, Pottbacker K, Woeltje M, Jahnen-Dechent W, Neuss S. Biomedical Materials. 2017; 12:4.
40. Wittmer CR, Claudepierre T, Reber M, Wiedemann P, Garlick JA, Kaplan D, Egles C. Advanced Functional Materials. 2011; 21:4232–4242.
41. Tsioris K, Raja WK, Pritchard EM, Panilaitis B, Kaplan DL, Omenetto FG. Advanced Functional Materials. 2012; 22:330–335.
42. Xia XX, Wang M, Lin Y, Xu Q, Kaplan DL. Biomacromolecules. 2014; 15:908–914. [PubMed: 24527851]
43. Wang XQ, Yucel T, Lu Q, Hu X, Kaplan DL. Biomaterials. 2010; 31:1025–1035. [PubMed: 19945157]
44. Kim S, Mitropoulos AN, Spitzberg JD, Tao H, Kaplan DL, Omenetto FG. Nature Photonics. 2012; 6:817–822.
45. Gogurla N, Sinha AK, Naskar D, Kundu SC, Ray SK. Nanoscale. 2016; 8:7695–7703. [PubMed: 26996157]
46. Gogurla N, Kundu SC, Ray SK. Nanotechnology. 2017; 28:10.
47. Tseng P, Zhao S, Golding A, Applegate MB, Mitropoulos AN, Kaplan DL, Omenetto FG. Acs Omega. 2017; 2:470–477. [PubMed: 30023608]
48. Kim DH, Lu NS, Ma R, Kim YS, Kim RH, Wang SD, Wu J, Won SM, Tao H, Islam A, Yu KJ, Kim TI, Chowdhury R, Ying M, Xu LZ, Li M, Chung HJ, Keum H, McCormick M, Liu P, Zhang YW, Omenetto FG, Huang YG, Coleman T, Rogers JA. Science. 2011; 333:838–843. [PubMed: 21836009]
49. Tarakanova A, Huang WW, Qin Z, Kaplan DL, Buehler MJ. Acs Biomaterials Science & Engineering. 2017; 3:2889–2899.
50. Ling SJ, Qin Z, Huang WW, Cao SF, Kaplan DL, Buehler MJ. Science Advances. 2017; 3:e1601939. [PubMed: 28435877]

## Biographies

Dr. Wenwen Huang is a postdoctoral associate in a joint program between the Department of Biomedical Engineering at Tufts University and Civil and Environmental Engineering at MIT, with the financial support of NIH. She received her bachelor’s degree in Physics from Peking University, Beijing, China, and her PhD in Physics from Tufts University. Her research interests include genetic engineering of hierarchical and stimuli-responsive proteins, physical and chemical modification of protein-based materials, as well as protein self-assembly mechanisms.

Dr. Shengjie Ling is an assistant professor in School of Physical Science and Technology at ShanghaiTech University. He is also a research affiliate at MIT and Tufts University. He obtained his B.S. from the Zhejiang University of Technology (2009) and PhD from Fudan University (2014). During 2012–2013, He awarded the State Scholarship Fund to pursue his study at ETH Zurich, Switzerland, as a joint PhD student. He did a postdoc training at MIT and Tufts University before joining ShanghaiTech University in September 2017.

Dr. Chunmei Li obtained her PhD in Chemical Engineering at Tufts University. After her postdoc training at Swiss Federal Institute of Technology at Zurich (ETH) and Tufts University, she is currently a research assistant professor in biomedical engineering department at Tufts university. Her research interests focus on the development of biomaterials for various biomedical applications, specifically novel protein-based materials for orthopedic application, biomaterials to regulate immune response, as well as scaffolding materials to create complex tissue microstructures.

Prof. Fiorenzo G. Omenetto is the Frank C. Doble Professor of Engineering, and a Professor of Biomedical Engineering at Tufts University. He also holds appointments in the Department of Physics and the Department of Electrical Engineering. His research interests are at the interface of technology, biologically inspired materials and the natural sciences with an emphasis on new transformative approaches for sustainable materials for high-technology applications. He also serves as Dean for Research for the School of Engineering.

Prof. David Kaplan holds an Endowed Chair, the Stern Family Professor of Engineering, at Tufts University. He is Professor & Chair of the Department of Biomedical Engineering and also holds faculty appointments in the School of Medicine, the School of Dental Medicine, Department of Chemistry and the Department of Chemical and Biological Engineering. He directs the NIH P41 Tissue Engineering Resource Center (TERC) that involves Tufts University and Columbia University and is Editor for the ACS Biomaterials Science and Engineering.

**Key Learning Points**

1. Silk amino acid sequence-structure relationships related to hierarchical structures
2. Silk protein designs and synthesis
3. Key top-down and bottom-up nanofabrication technologies for silk-based materials
4. Application of silk-based materials in bio-nanotechnology: tissue regeneration and drug delivery
5. Application of silk-based devices in bio-nanotechnology: optics, electronics, sensors and filtration

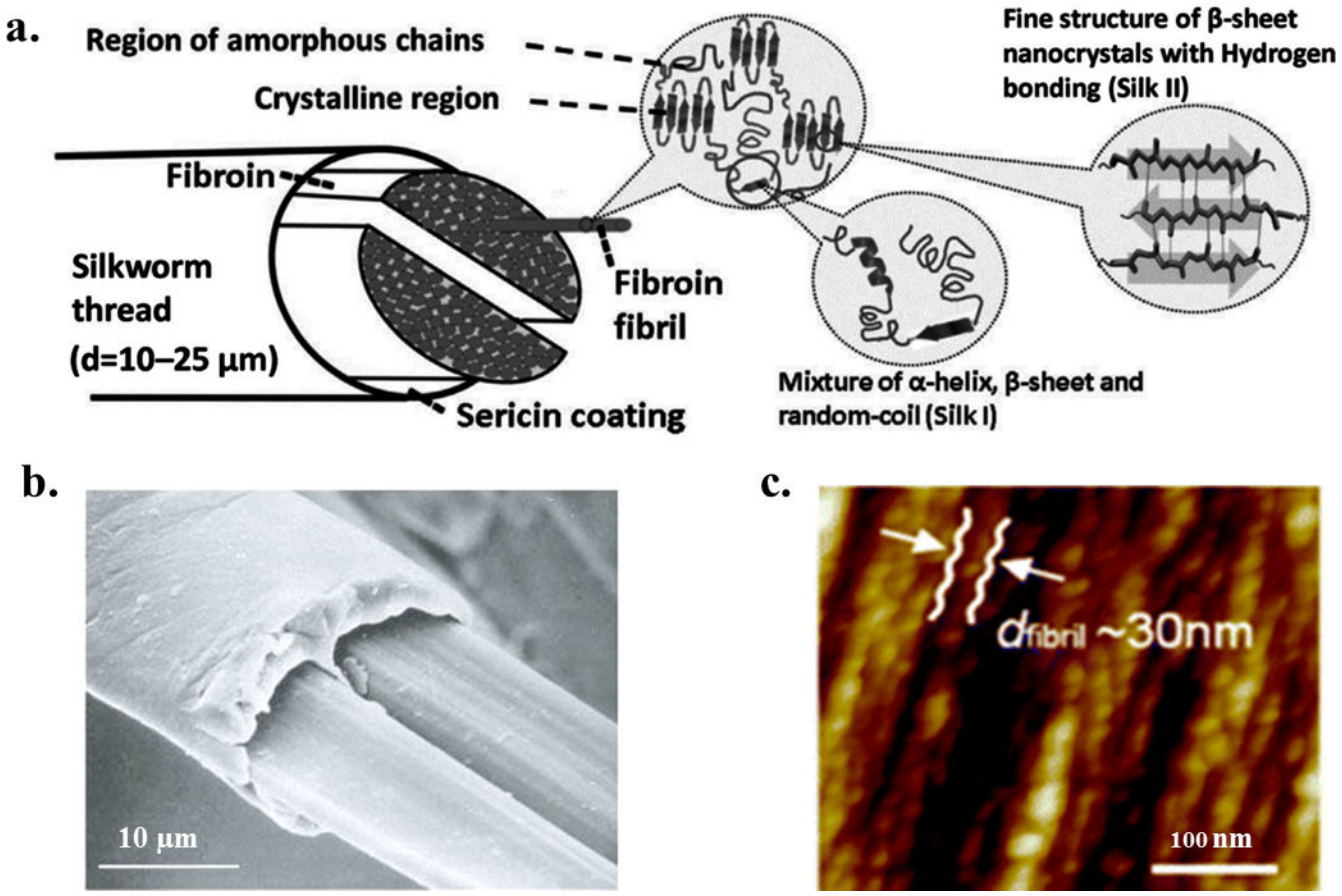


**Figure 1. Hierarchical structure of *B. mori* silk**

(a) *B. mori* silk fiber has a core-shell type structure, with silk fibroin as the inner core and sericin as the outer coating. Each silk fibroin brin is composed of numerous interlocking fibroin fibrils. Inside the fibroin fibrils, the β-sheet nanocrystals are connected by amorphous chains to form a heteronanocomposite. β-sheet nanocrystals are composed of stacked β-sheets with peptide chains connected by hydrogen bonds in each sheet. The lattice constants of the orthogonal unit cell of β-sheet nanocrystal are a = 0.938 nm, b = 0.949 nm, and c = 0.698 nm for silkworm, *B. mori,* silk. (b) Scanning electron microscopy image of native *B. mori* silkworm silk (scale bar: 10 μm). (c) Atomic force microscopy image of the fibroin fibril structure in *B. mori* silkworm silk with a sequence of linked segments (scale bar: 100 nm). Adapted with permission from refs 7, 8 and 9. Copyright 2002 Springer Nature, 2013 Royal Society of Chemistry, and 2017 MDPI AG, Basel, Switzerland.

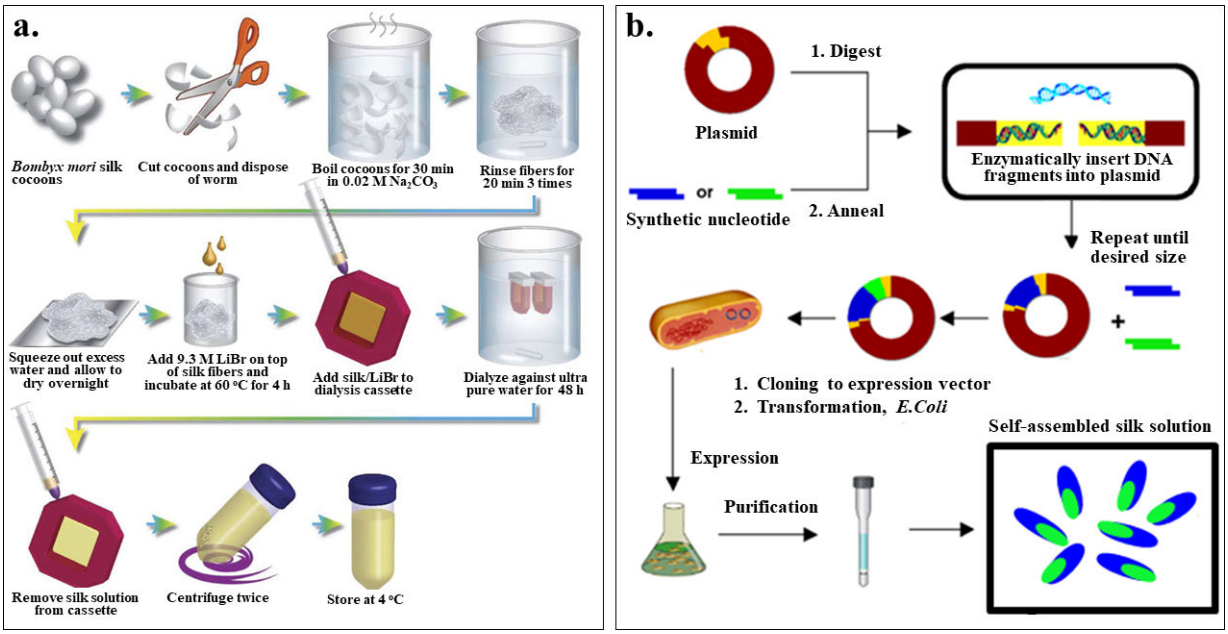


**Figure 2. Production of silk protein solutions**

Generating silk protein solutions is essential for their applications as functional materials. Among various silk protein synthesis methods, two methods are industrially scalable: silk fibroin extraction and bioengineered silk fermentation. (a) Schematic of the silk fibroin extraction procedure for the production of *B. mori* regenerated silk fibroin (RSF). (b) General biosynthesis scheme of bioengineered silks using recombinant DNA technology. Adapted with permission from refs 2 and 19. Copyright 2011 Springer Nature, and 2015 Springer Nature.

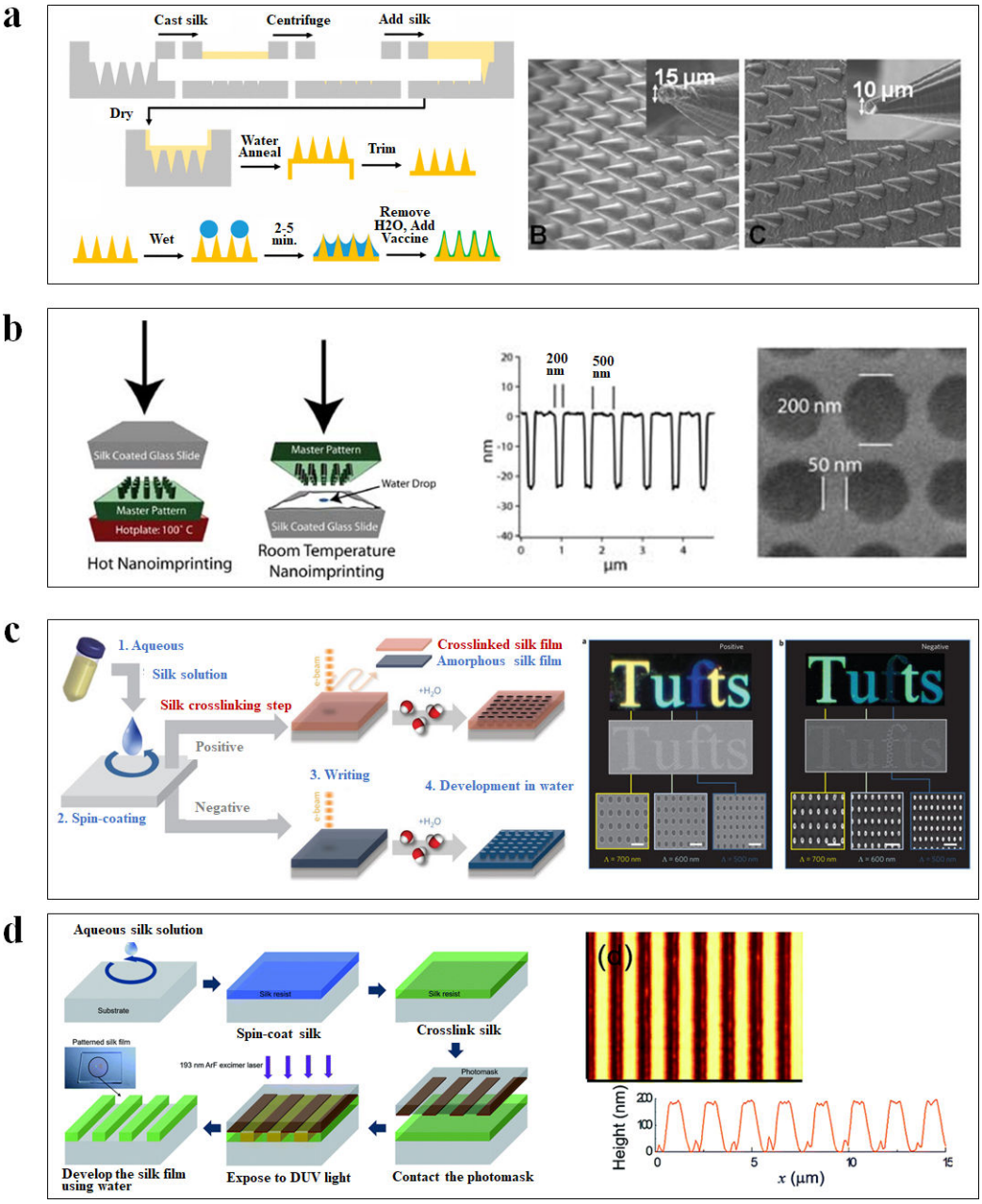


**Figure 3. Lithography of silk-based biomaterials**

(a) Schematic of soft lithography for vaccine-coated silk fibroin microneedles. SEM images of cone shaped microneedles prepared from an aqueous silk solution with different shapes and geometries. (b) Schematic diagrams of two nanoimprinting processes: hot embossing and room-temperature embossing. SEM image of a silk film imprinted with a periodic array of 200 nm diameter 30 nm height chromium nanoparticles separated by 250 nm. (c) Schematic of all-water-based electron-beam patterning on a silk film. Dark-field and electron microscopy images of silk nanostructures generated on positive and negative resist. (d) Schematic diagrams showing the ArF excimer laser photolithography process to form high-resolution silk fibroin micropatterns. Atomic force microscopy image of the patterned

silk suggested the feature was around 190 nm in height and 1 μm in line width. Adapted with permission from refs 21, 23, 26, 27 and 28. Copyright 2010 WILEY-VCH, 2013 WILEY-VCH, 2014 Springer Nature, 2016 The Royal Society of Chemistry and 2017 American Chemical Society.

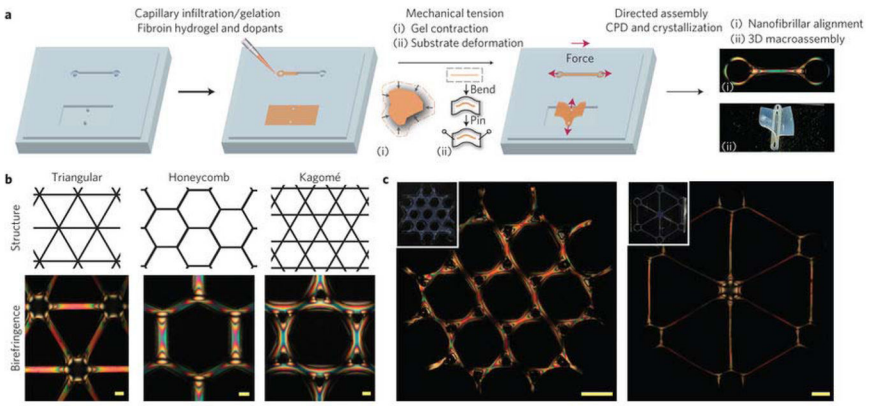


**Figure 4. Mechanical tension-mediated formation of patterned nanofibrillar structure**

(a) General schematic of the directed assembly protocol. Aqueous silk fibroin is mixed with crosslinkers hydrogen peroxide and horseradish peroxidase and infiltrated/gelled in a PDMS mold. Mechanical tension is subsequently introduced by either contraction of the gel in mixtures of ethanol and water, or direct deformation of the elastomeric substrate. Finally, as the structures undergo critical point drying (CPD), β-sheet physical crosslinking in the silk is induced, stabilizing the material in its mechanically modified state. The final structure possesses tension-engineered nano-, micro- and macrostructure. b, Birefringence of sample microscale, nanofibrillar unit cells generated from periodic shapes. Scale bars, 100 μm. (c) Large-scale structures composed of tri-hexagonal and triangular components. Inset: camera images of the whole structure taken under diffuse white light. Scale bars, 1 mm. Adapted with permission from ref 29. Copyright 2017 Springer Nature.

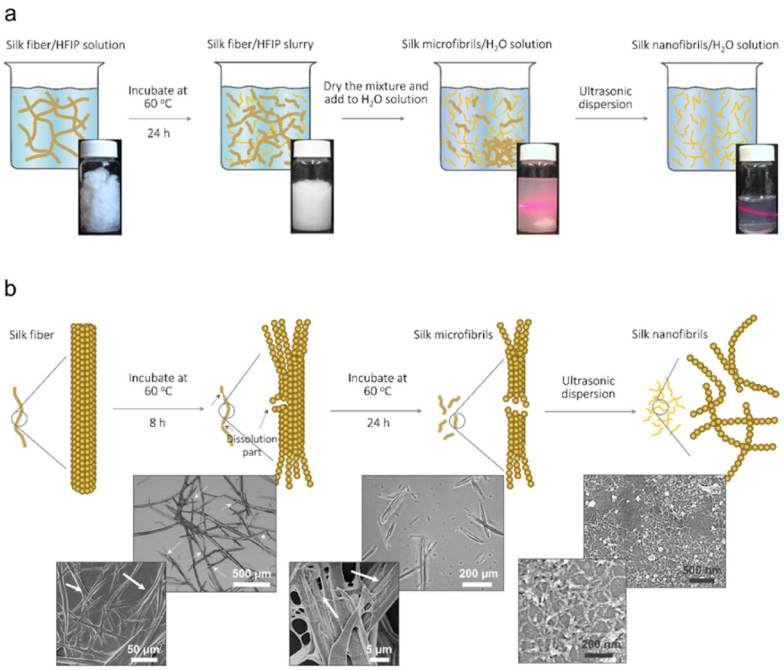


**Figure 5. Liquid exfoliation process of silk fiber**

(a) Schematic and photographs showing the fabrication steps and their relevant solution. Step 1: silk fiber immersed in hexafluoroisopropanol (HFIP) solution with a weight ratio of 1:30 and the mixture was incubated for 24 h to obtain silk fiber/silk microfibers (SMFs) slurries. Step 2: the dried silk fiber slurries were transferred to $H_2O$ solution and the silk fiber precipitation was removed to gain SMFs dispersion. Step 3: the SNFs dispersion was prepared via ultrasonic treatment. (b) Schematic (top row) of liquid exfoliation of silk fiber and representative optical microscopy (the first two images in middle row) and scanning electron microscopy (SEM; the third image in middle row, and the images in bottom row) images of resultant products in each process. Silk fiber was dissolved by HFIP from the defect and ends and can be split to SMFs after 24 h. The white arrows in the optical microscopy and SEM images show the dissolution of silk fibers and SMFs. The SNFs with a diameter of 20 ± 5 nm are obtained after ultrasonic dispersion (SEM images in the last column). Adapted with permission from ref 30. Copyright 2016 WILEY-VCH.

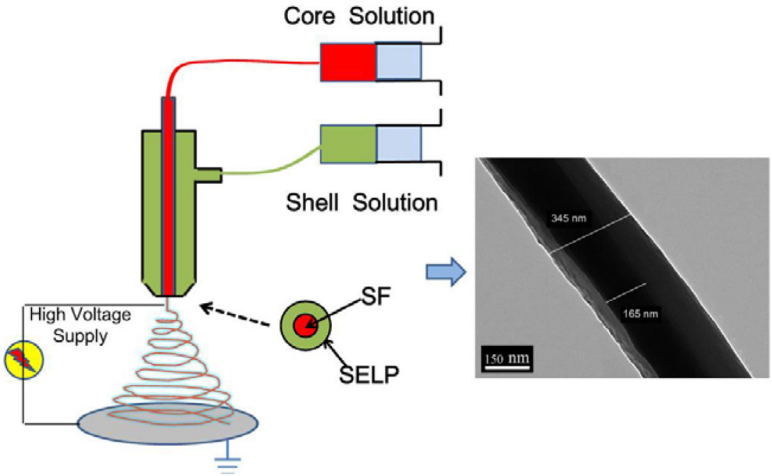


**Figure 6. All-aqueous coaxial electrospinning process**

In this process, silk fibroin (SF) and silk-elastin-like protein polymer (SELP), both in aqueous solution and with high and low viscosity, respectively, were used as the inner (core) and outer (shell) layers of the nanofibers. The electrospun SF core solution served as a spinning aid for the nonelectrospinnable SELP shell solution. Uniform nanofibers with average diameters from 301 ± 108 nm to 408 ± 150 nm were obtained by adjusting processing parameters. Adapted with permission from ref 31. Copyright 2016 MDPI AG, Basel, Switzerland.

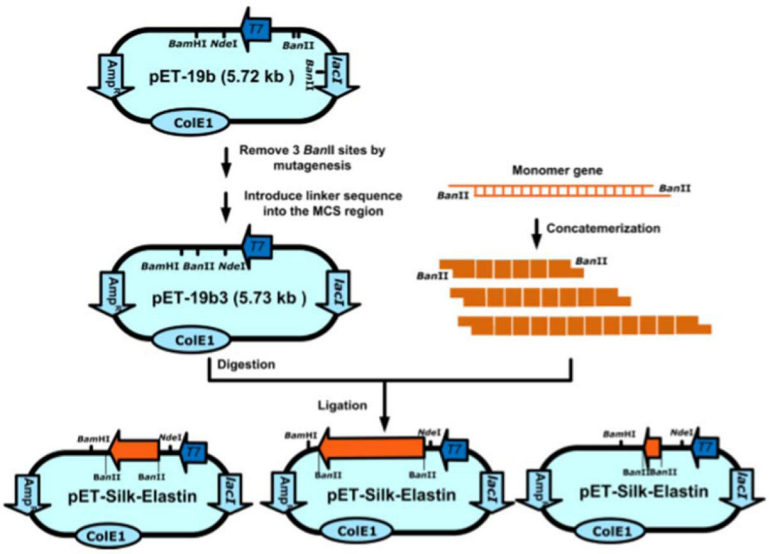


**Figure 7. Construction of expression plasmids for recombinant silk elastin-like protein polymers**

Multimerization of the silk monomer through "concatemerization" relying on the BanII restriction enzyme site. Adapted with permission from ref 14. Copyright 2011 American Chemical Society.

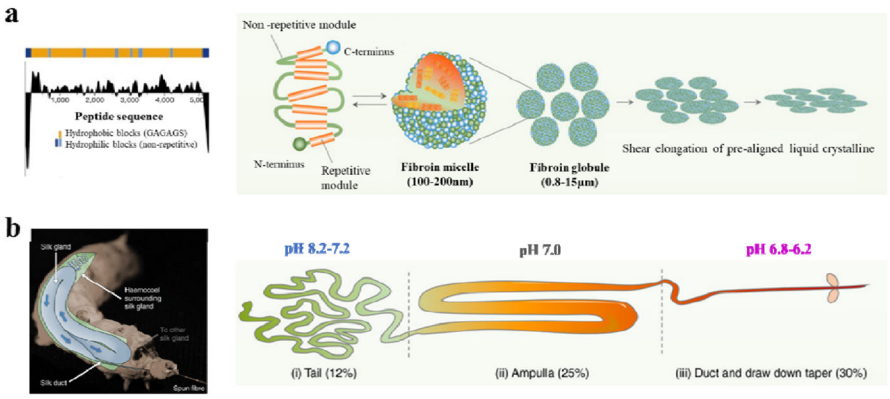


**Figure 8. Self-assembly of silk fibroin micelles during spinning process**

(a) Hydrophobicity pattern in *B. mori* silk fibroin heavy chain primary sequence and schematic model of the natural silk fiber assembly mechanism during the spinning processes. (b) Anatomical overview and illustration of the *B. mori* silk gland. The silkworm spinning gland is divided into three regions. The silk proteins are synthesized in the tail and transferred to the ampulla with increased concentration. In this region, the silk proteins are assembled to micelle-like structures with anisotropic liquid-crystalline properties. Finally, silk fiber formation occurs at decreased pH, shear stress and dehydration during pulling of the nematic silk proteins from the spigot (by the head motion of the worm). Adapted with permission from refs 33, 34 and 35. Copyright 2003 Springer Nature and 2017 Springer Nature.

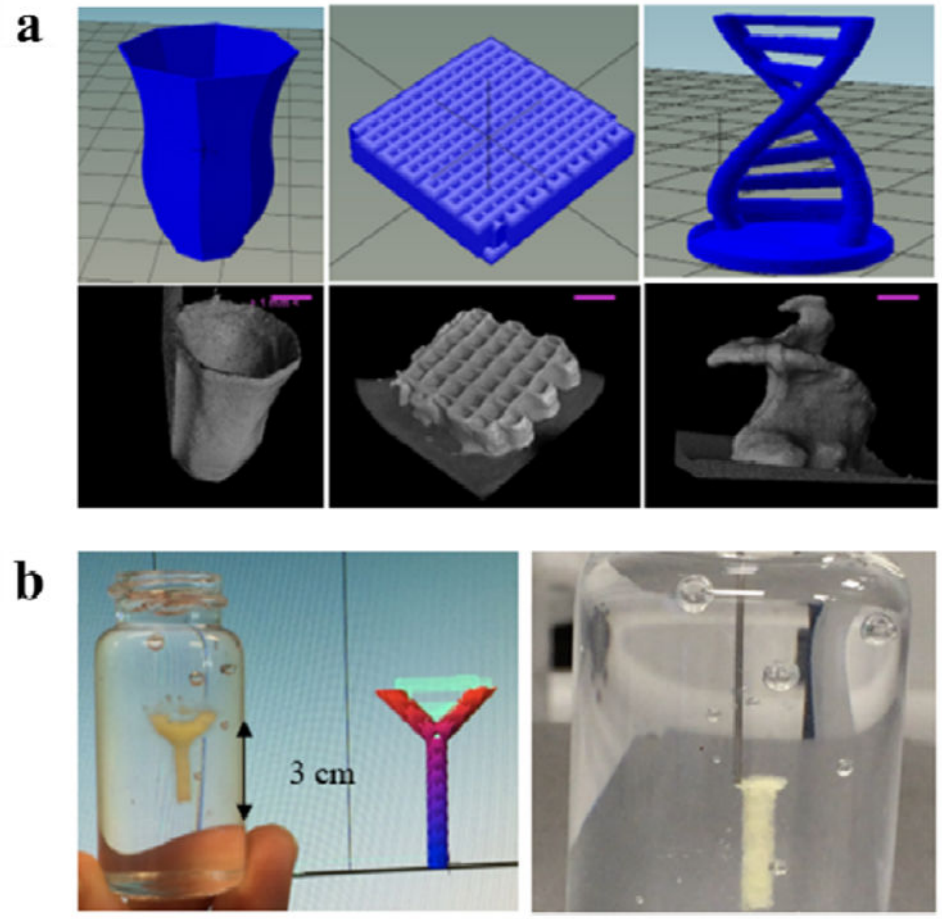


**Figure 9. 3D printing of silk fibroin**

(a) Design of printed structures (top) and CT-scan images of printed structures (bottom) showing hollow structure (vase) tissue scaffold and free-standing object (helix). Scale bars in A represent 1 mm. (b) Printed structure inside Nano-clay granular gel medium and image showing printing process (right). Adapted with permission from ref 36. Copyright 2018 Elsevier Ltd.

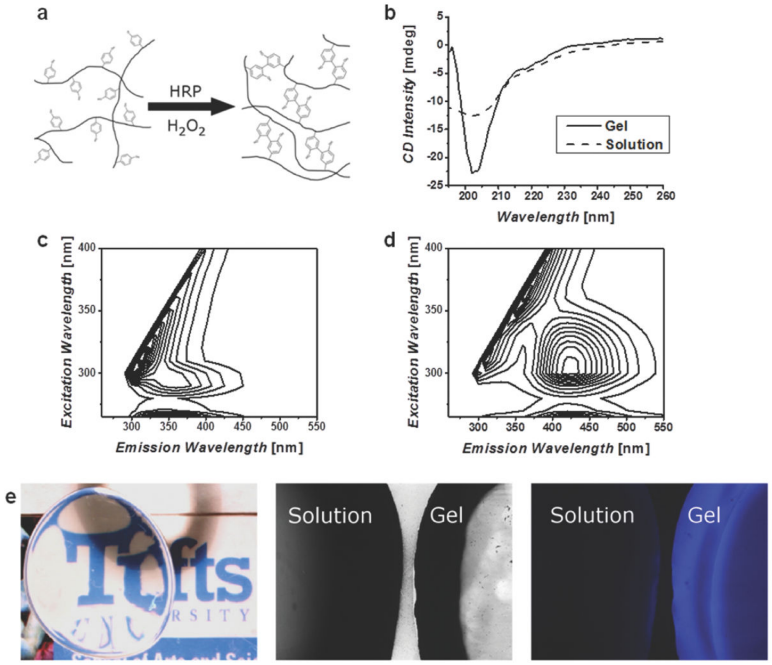


**Figure 10. Enzyme catalyzed chemical crosslinking of silk fibroin**

(a) Schematic representation of the crosslinking of tyrosine residues on silk molecules, these covalent bonds allow for chain extension creating highly elastic hydrogels. (b) Circular dichroism (CD) spectra of silk solution and enzymatically formed hydrogels, show a change to a helical structure and not β-sheet as found in other silk materials. Fluorescence excitation-emission spectra of (c) solution and (d) gel confirm the formation of dityrosine bonds. (e) The resultant hydrogels are optically clear and exhibit a blue fluorescence when irradiated with UV that is not present in the precursor solution. Adapted with permission from ref 38. Copyright 2014 WILEY-VCH.

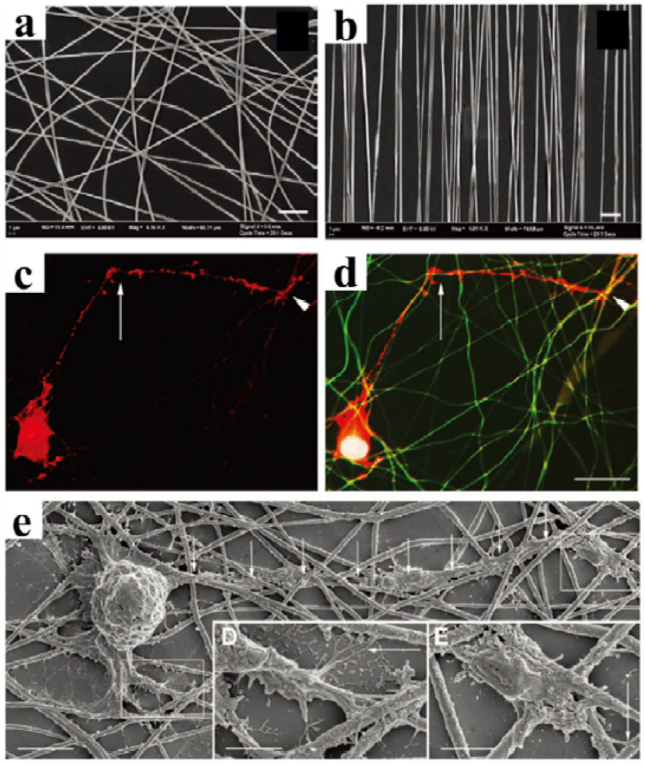


**Figure 11. Silk nanofibers for central nerves regeneration**

The alignment of electrospun silk fibers depended on the speed of the rotating wheel collector: (a) fibers spun at static condition 0 m/s showing no alignment, and (b) fibers spun at 10 m/s showing optimal alignment. Scale bars: 5 μm. Retinal ganglion cells (RGC) culture on silk nanofibers: (c) phalloidin labelling of the actin filaments in RGC shows a neurite exhibiting a sharp change in direction of growth (arrow), while (d) merged image composed of the tetramethylrhodamine (TRITC) phalloidin (red), 4′,6-diamidino-2-phenylindole (DAPI) nuclear staining (blue) and autofluorescence (green) of the silk network demonstrates that the growth cone (the arrowheads in c and d) elongates in contact with silk fibers and that the sharp changes of direction correspond to silk crossroads (arrows in c and d). (e) SEM of RGC reveals that neurons grow in close contact with the silk. Adapted with permission from ref 40. Copyright 2011 WILEY-VCH.

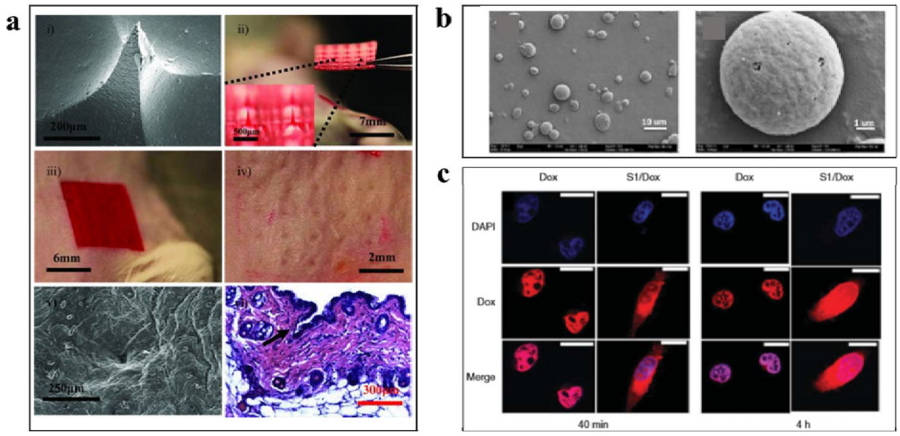


**Figure 12. Silk-based biomaterials for drug delivery**

(a) Silk microneedles as applied to mouse skin: i) scanning electron micrograph of an individual silk microneedle, ii) silk microneedles patch, relative size comparison to mouse, iii) silk microneedles patch applied to animal skin, iv) skin after removal of microneedles patch, needle penetration marks are clearly visible, v) scanning electron micrograph of penetrated skin, and, vi) histology section of individual indentation site – epidermis was breached (arrow) allowing access to the underlying tissue; successful penetration of skin demonstrates sufficient mechanical strength of silk microneedles.(b) Silk microparticles: scanning electron microscopic images of silk particles prepared from 1/4 mass ratio silk/PVA blend films. (c) Silk nanoparticle: doxorubicin delivery into HeLa cells using SELP nanoparticles at: (A) 40 min and (B) 4 h incubation time. Adapted with permission from refs 41, 42 and 43. Copyright 2010 Elsevier Ltd, 2011 WILEY-VCH, and 2014 American Chemical Society.

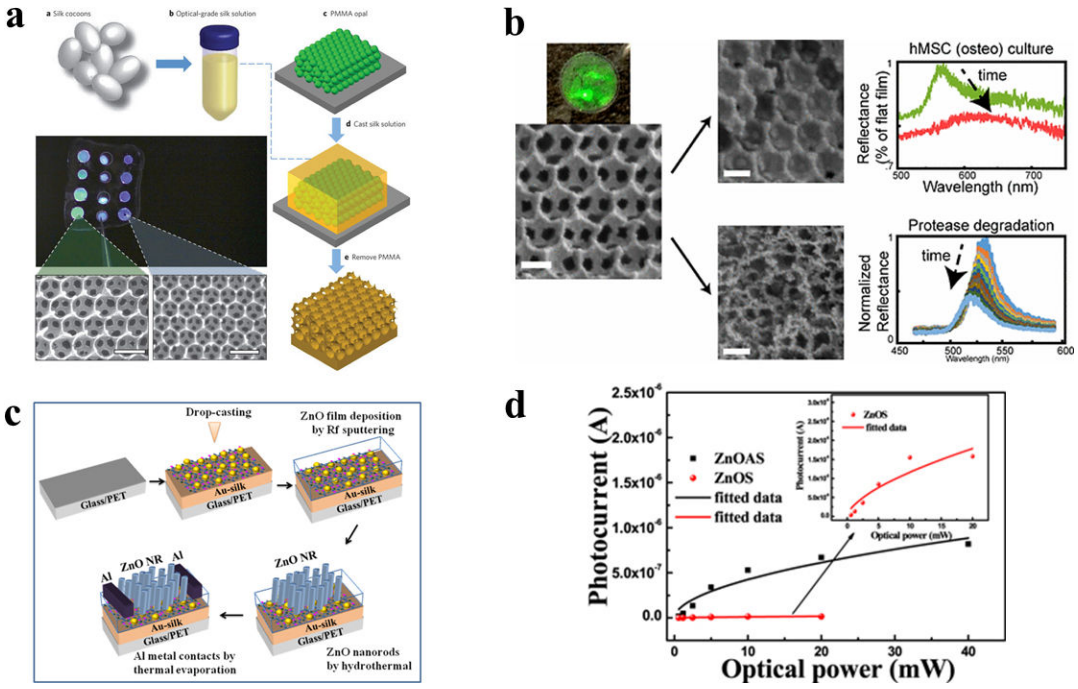


**Figure 13. Silk inverse opals for smart cell culture**

(a) Fabrication process for inverse opals. (b) Silk inverse opal degradation in response to a protease. Reflectance over time during the incubation of opals in protease XIV. (c) Fabrication process for lateral ZnO NRA photodetectors on Au-silk protein coated glass substrates. (d) Photocurrent as a function of incident optical power measured at 5 V for ZnOAS and ZnOS devices. Adapted with permission from refs 44, 46 and 47. Copyright 2012 Springer Nature, 2017 IOP Publishing Ltd and 2017 American Chemical Society.

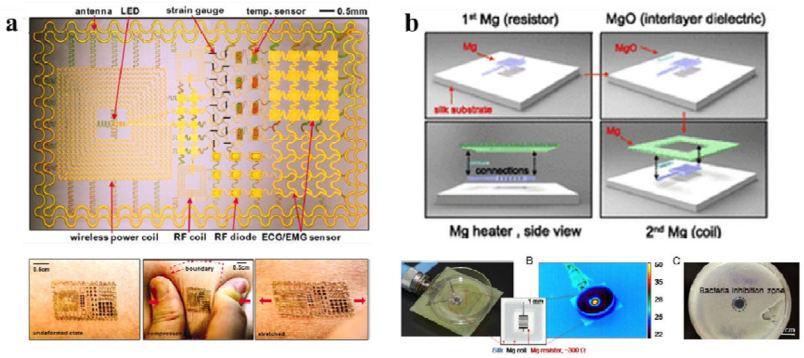


**Figure 14. Silk-based flexible electronics**

(a) Epidermal Electronics. Image of a demonstration platform for multifunctional electronics with physical properties matched to the epidermis. Mounting this device on a sacrificial, water-soluble film of PVA, placing the entire structure against the skin, with electronics facing down, and then dissolving the PVA leaves the device conformally attached to the skin through van der Waals forces, in a format that imposes negligible mass or mechanical loading effects on the skin. (b) Silk-based resorbable wireless heating devices for therapy and drug release. Schematic of the wireless heating device integrated with drug-loaded silk. The heating device comprises a resistor and a wireless coil encapsulated in silk fibroin. Drug molecules loaded in the silk film can be triggered to release under heat treatment for bacterial inhibition. Adapted with permission from refs 20 and 48. Copyright 2011 American Association for the Advancement of Science and 2014 National Academy of Sciences USA.

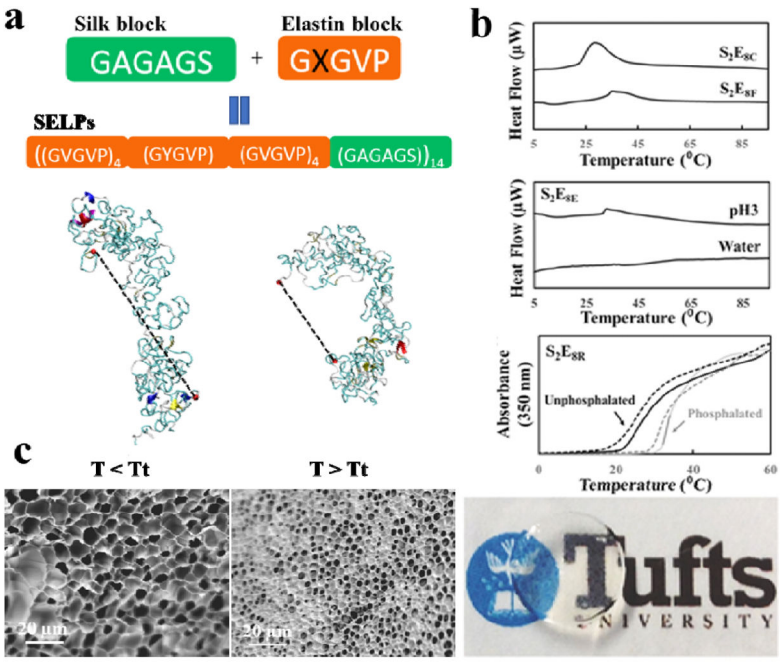


**Figure 15. Silk-elastin-like protein dynamic hydrogels**

**(a)** SELP sequences and representative structures from simulation, at (i) 7 and (ii) 57°C. Dotted lines represent end-to-end molecular distance. **(b)** SELPs respond to temperature, a physical stimulus, exemplified by SELP with cysteine and phenylalanine mutation in the elastin domains, S2E8C and S2E8F; SELPs respond to pH, a chemical stimulus, exemplified by SELP with glutamic acid mutation in the elastin domains, S2E8E; and SELPs respond to phosphorylation, a biological stimulus, exemplified by with arginine mutation in elastin domains, S2E8R. (c) SEM images showing the micromorphology changes of S2E8R hydrogel samples in swollen states at 4°C (<LCST) and in contracted states at 37°C (>LCST) in deionized water. Adapted with permission from refs 18 and 49. Copyright 2016 WILEY-VCH and 2017 American Chemical Society.

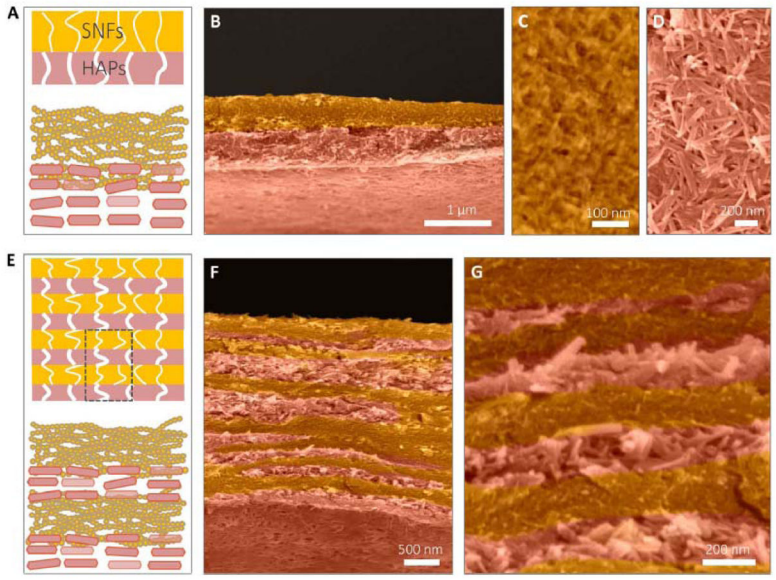


**Figure 16. Silk-based multilayer filtration system**

The double-layer structure of the SNF/HAP membranes was formed through vacuum filtration of 1 ml of SNF/HAP dispersion. (A) Schematic of double-layer structures. The top layer is the SNF-rich layer with small pore sizes. The bottom layer is the HAP layer with larger pore sizes. (B) Cross-sectional SEM image of a double-layer membrane. (C and D) Top-view SEM images of SNF-rich (C) and HAP-rich (D) layers. (E to G) The multilayer structure of the SNF/HAP membrane was generated from 3-ml SNF/HAP dispersion using a 3.5-cm-diameter mold. (E) Schematic of multilayer structures. (F) Cross section SEM image of a multilayer membrane. (G) High-resolution cross-sectional SEM image of a multilayer membrane. Adapted with permission from ref 50. Copyright 2017 American Association for the Advancement of Science.

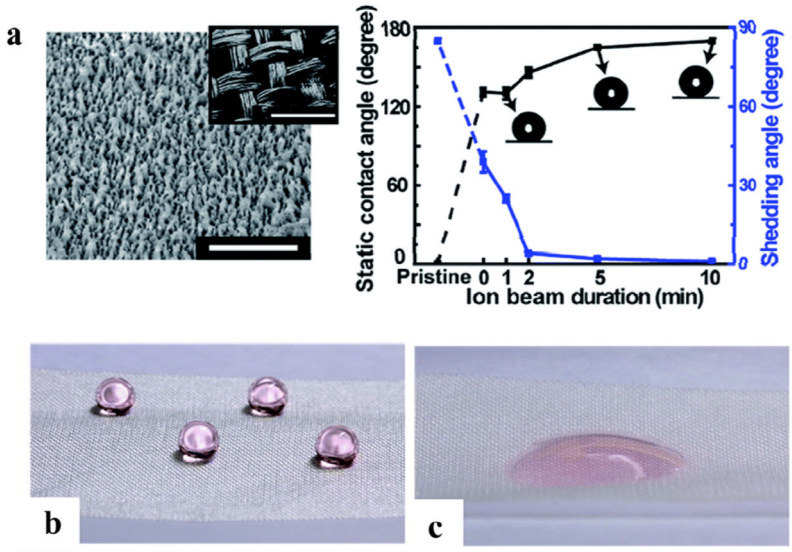


**Figure 17. Super-hydrophobic silk fabrics**

(a) SEM images of nanostructures formed on a silk fabric exposed by ion beam treatment. The inset in shows micro-scale woven structures of the silk fabric. The scale bars are 1 μm and 400 μm. Static contact angle (black line) and shedding angle (blue line) of a water droplet measured after 30 s of hydrophobic coating with various ion beam durations. (b) The ion beam treated surface and (c) untreated surface of the same fabric maintaining super-hydrophobicity and hydrophilicity, respectively. Adapted with permission from ref 24. Copyright 2014 Royal Society of Chemistry.

**Table 1**

Tensile mechanical properties of silks and other materials (adapted from ref. 4, 5, 11).

| **Materials** | **Stiffness [GPa]** | **Strength [MPa]** | **Extensibility [%]** | **Toughness [MJ m$^{-3}$]** |
|---|---|---|---|---|
| *B.mori* silk (with sericin) | 5–12 | 500 | 19 | 70 |
| *B. mori* silk (without sericin) | 15–17 | 610–690 | 4–16 | 70–78 |
| *N. clavipes* silk | 11–13 | 875–972 | 17–18 | 111–160 |
| *N. clavipes* silk (285kDa recombinant) | 21 | 508 | 15 | - |
| Bone | 20 | 160 | 3 | 4 |
| Collagen | 0.0018–0.046 | 0.9–7.4 | 24–68 | - |
| Elastin | 0.001 | 2 | 150 | 2 |
| Resilin | 0.002 | 3 | 190 | 4 |
| Synthetic rubber | 0.001 | 50 | 850 | 100 |
| Polylactic acid | 1.2–3.0 | 28–50 | 2–6 | 1–3 |
| Nylon fiber | 5 | 950 | 18 | 80 |
| Kevlar 49 fiber | 130 | 3600 | 2.7 | 50 |

**Table 2**

Mechanical data of various regenerated silk morphologies (adapted from ref. 13).

| Material formats | Stiffness [GPa] | Strength [MPa] | Extensibility [%] | Pore size [μm] (porosity [%]) |
|---|---|---|---|---|
| Films (as cast) | 3.9 | 47.2 | 1.9 | - |
| Films (methanol-treated) | 3.5 | 58.8 | 2.1 | - |
| Films (water-annealed) | 1.9 | 67.7 | 5.5 | - |
| Films (ultrathin, i.e., 20–100 nm; spin coating and spin-assisted layer-by-layer assembly) | 6–8 | 100 | 0.5–3 | - |
| Hydrogels (8% w/v) | - | 0.0252 | - | - |
| Electrospun mat (concentration of 3%, electric field of 1 kV/cm and 10–15 cm spinning distance) | - | 15 | 40 | - |
| Electrospun mat (concentration of 15%, electric field of 2 kV/cm and 5 cm spinning distance) | 0.515 | 7.25 | 3.2 | - |
| Methanol-treated sponges (concentration 6 wt%) | 0.00043 | 0.02 | - | 151 ± 40 (88%) |
| HFIP-derived sponges (concentration 17 w/v%) | 0.00045–0.001 | 0.175–0.25 | - | 15–202 |
| Aqueous-derived sponges (concentration 4 w/v%) | 0.00007 | 0.011 | - | 940 ± 50 (95%) |
| | 0.00008 | 0.011 | - | 760 ± 30 (95%) |
| | 0.0001 | 0.012 | - | 650 ± 30 (97%) |
| | 0.000115 | 0.013 | - | 570 ± 30 (97%) |
| | 0.00013 | 0.013 | - | 470 ± 30 (97%) |
| Aqueous-derived sponges (concentration 8 w/v%) | 0.0013 | 0.1 | - | 920 ± 50 (92%) |
| | 0.00153 | 0.125 | - | 750 ± 20 (94%) |
| | 0.00194 | 0.14 | - | 640 ± 30 (95%) |
| Aqueous-derived sponges (concentration 10 w/v%) | 0.00333 | 0.32 | - | 920 ± 50 (85%) |